

Review

Molten salt synthesis of lead-based relaxors

KI HYUN YOON, YONG SOO CHO*, DONG HEON KANG‡

Department of Ceramic Engineering, Yonsei University, Seoul 120-749, Korea

E-mail: khyoon@bubble.yonsei.ac.kr

The molten salt synthesis (MSS) of lead-based relaxors which have a perovskite structure, $A(B^I B^{II})O_3$ where B^I is Mg^{2+} , Fe^{3+} , Zn^{2+} , Ni^{2+} or Co^{2+} , and B^{II} is Nb^{5+} , has been reviewed with regard to the formation of the perovskites, phase stability and morphology characteristics. Two relaxor materials, $Pb(Mg_{1/3}Nb_{2/3})O_3$ and $Pb(Fe_{1/2}Nb_{1/2})O_3$ were found to be successfully synthesized at a low temperature in a very short time by the MSS method. Using the example of $Pb(Mg_{1/3}Nb_{2/3})O_3$, the phase stability has been discussed on the basis of thermal and chemical analyses. The influences of the processing parameters, such as temperature, time, type and amount of salt, and non-stoichiometry, on the formation and the powder characteristics of the perovskite phase were investigated with possible explanations for the observed differences which were induced by changing the parameters. Finally, densification behaviour and dielectric properties resulting from the MSS powder were examined and compared to those of powders obtained by using the conventional mixed oxides (CMO) method. © 1998 Kluwer Academic Publishers

1. Introduction

Several novel processing methods for ceramic powder preparation have been introduced to overcome the problems present in the conventional methods. The molten salt synthesis (MSS) method is one of the simplest methods for obtaining highly reactive powders of a single phase at low temperatures in a shorter soaking time, in which the molten salt is used as a reaction aid [1–4]. Various electronic ceramics, such as $BaTiO_3$ [5–9], $Y_1Ba_2Cu_3O_{7+\delta}$ [10], $Bi_4Ti_3O_{12}$ [11], ferrites [12–15], $Pb(ZrTi)O_3$ [16] and lead-based niobates [17–21] have been studied by adjusting the MSS method using chlorides, sulphates or carbonates. The powders obtained by the MSS method have several unique characteristics compared to those obtained by other methods such as the conventional mixed oxides (CMO); coprecipitation and sol-gel methods, which are determined mainly by the chemical and crystallographic constraints given by the salt [1, 19]. The features are more distinguishable in the case of strongly anisotropic materials. It is believed that the features are related to the surface and interface energies between the constituents and the salt, resulting in a tendency to minimize the energies by forming a specific morphology. The environments during the development of the morphology can be controlled by an appropriate choice of salt. Therefore, the selection of salt is critical in obtaining desirable powder characteristics. There are several requirements for the selection of salt. First, the melting point of the salt should be low and appropriate for the synthesis

of the required phase. In many cases, several eutectic compositions have been used to reduce the melting point of the salt. The salt should possess sufficient aqueous solubility in order to eliminate the salt easily by washing after synthesis. The stability of the salt against any harmful interactions between the salt and the constituents can be another factor [1–16].

The lead-based relaxors, $Pb(Mg_{1/3}Nb_{2/3})O_3$ (PMN), $Pb(Fe_{1/2}Nb_{1/2})O_3$ (PFN), $Pb(Zn_{1/3}Nb_{2/3})O_3$ (PZN), $Pb(Ni_{1/3}Nb_{2/3})O_3$ (PNN) and $Pb-(Co_{1/3}Nb_{2/3})O_3$ (PCN) are very useful materials for applications of capacitors, actuators and transducers. The relaxors have a pseudocubic perovskite structure above the paraelectric-ferroelectric transition point, leading to a very small anisotropic nature during particle growth in the molten salt [16]. Fig. 1 shows the main processing stages of the MSS method with increasing temperature in the case of the lead-based relaxors. Oxides corresponding to a lead-based compound are mixed with one or two kinds of salt and then fired at a temperature above the melting point of the salt to form a flux of the salt composition. At this temperature, the oxides are rearranged and then diffused rapidly in a liquid state of the salt. With further heating, particles of the perovskite phase are formed through the nucleation and growth processes.

It is known that usually, the reaction mechanism of a given phase in the MSS is little different from that of the solid-state reaction, as long as the salt intervenes in the formation reaction of the required phase. For example, in the case of PFN, different reaction

* Present address: New York State College of Ceramics at Alfred University, Alfred, NY 14802, USA.

‡ Present address: Department of Electronic Materials Engineering, The University of Suwon, Suwon 445-743, Korea.

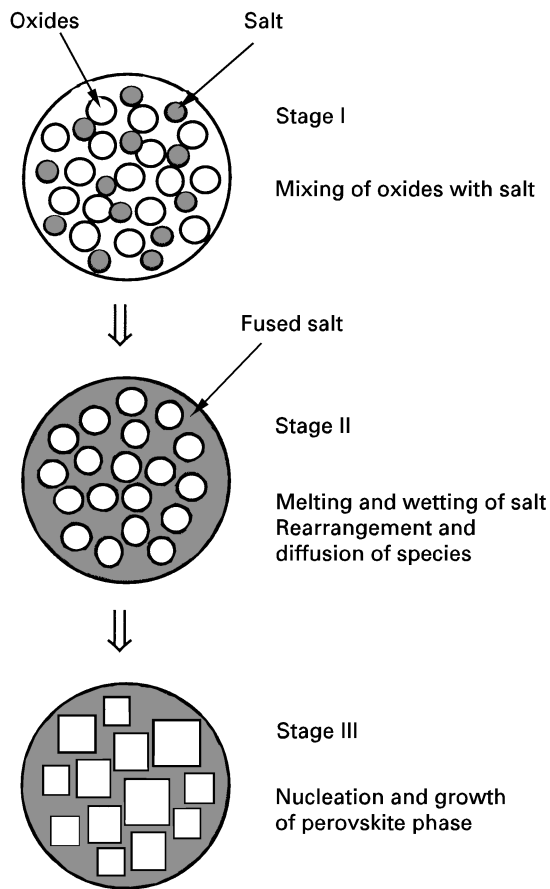


Figure 1 Schematic illustration of the MSS process with increasing temperature.

mechanisms have been reported in the two methods, MSS and CMO [20,21]. These results are mainly related to the different reaction routes affected by the instability of salt, and the pyrochlore-type intermediate phases such $Pb_3Nb_4O_{13}$, $Pb_2Nb_2O_7$ and $Pb_3Nb_2O_8$.

The experimental procedure for the MSS method is shown in Fig. 2. Usually, oxides corresponding to the lead-based relaxor composition are used as raw materials. The oxides are ball-mixed with salts which are appropriate for a given material. The synthesis of the perovskite phase can be conducted above the melting point of the selected salt within a very short time. After cooling, the salt is eliminated by washing with deionized water. Through a careful drying step, unagglomerated MSS powders can be obtained. It is noticeable that the MSS procedure is very simple and cost-effective, compared with the other chemical methods.

There are many experimental parameters in the MSS, which influence the resulting powder characteristics and the reaction kinetics. Table I summarizes the processing parameters and their influences on the reaction rates and morphology characteristics. Fig. 2 also shows the factors at each experimental step which possibly influence the final powder characteristics. The synthesis temperature and time are the usual factors which lead to different results. Changes in the amount and type of salt can induce a huge difference in powder characteristics because they are responsible for the reaction and growth environments. The anion size of the salt, the solubilities of the constituents in the

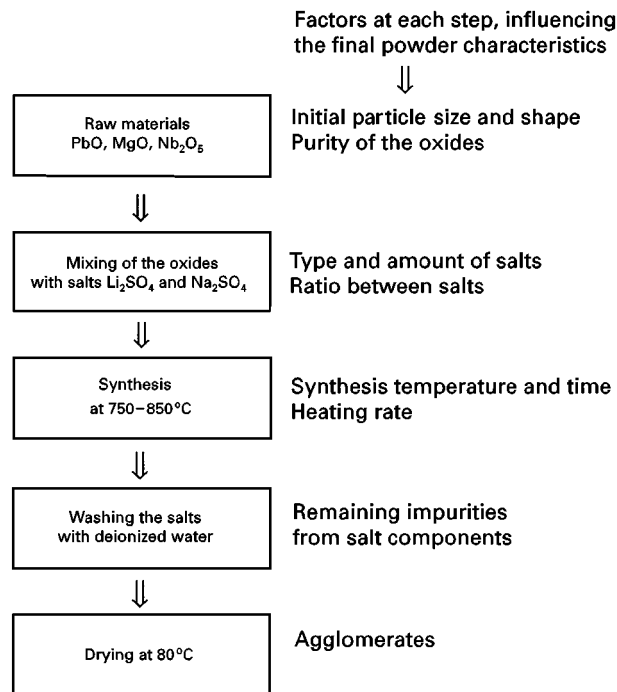


Figure 2 Flow chart and factors influencing the MSS method for PMN synthesis using Li_2SO_4 and Na_2SO_4 .

TABLE I Effects of processing parameters in the MSS on reaction rate and powder characteristics: (○) predominantly dependent, (×) less dependent

Processing parameters	Reaction rate	Particle size	Particle shape
Temperature	○	○	○
Time	×	○	○
Amount of salt	×	○	×
Type of salt			
Anion size	×	○	○
Solubility effect	○	○	○
Difference in m.p.	○	×	×
Ratio between salts ^a	○	×	×
Excess PbO	×	×	○

^a When using two different salts.

salt and the melting point of the salt, as well as the niobate composition and initial particle size can also be considered as influencing factors. The effects of the processing parameters on the reaction rate and particle morphology characteristics of the lead-based materials are the main topics of this review. Mainly, PMN will be used to explain the results according to the parameter changes because it has proved to be more stable in molten salts than the other relaxors.

2. Formation of the perovskite phase

The formation of the perovskite phase can take place at much lower temperatures in the MSS than in the CMO. For example, a temperature of 750°C is needed to form a pure PMN phase in sulphate MSS compared with 1100°C for CMO PMN. This can be attributed mainly to the enhanced diffusivity of the constituent oxides in the liquid state of the salt.

Table II shows the results of phase analysis in the lead-based materials fired at 750°C. The PMN and

TABLE II Analysis of phases present in lead-based relaxors fired at 750 °C for 1 h with variation in salt species

Compositions	Salts ^a	Perovskite phase (%)	Pyrochlore phase (%)
Pb(Mg _{1/3} Nb _{2/3})O ₃	KCl	73	27
	NaCl–KCl	86	14
	NaCl–LiCl	0	20 ^b
	Li ₂ SO ₄ –Na ₂ SO ₄	98	2
Pb(Fe _{1/2} Nb _{1/2})O ₃	NaCl–KCl	93	7
	Li ₂ SO ₄ –Na ₂ SO ₄	91	9
Pb(Zn _{1/3} Nb _{2/3})O ₃	NaCl–KCl	9	91
	Li ₂ SO ₄ –Na ₂ SO ₄	6	94
Pb(Ni _{1/3} Nb _{2/3})O ₃	NaCl–KCl	11	89
	Li ₂ SO ₄ –Na ₂ SO ₄	21	79
Pb(Co _{1/3} Nb _{2/3})O ₃	NaCl–KCl	9	91
	Li ₂ SO ₄ –Na ₂ SO ₄	8	92

^a Ratios between two salts correspond to their eutectic compositions.

^b With unknown phases.

PFN phases were effectively synthesized at 750 °C by the MSS. All compositions, except in the case of NaCl–LiCl, were observed to consist of the perovskite phase and the pyrochlore phase. The amount of perovskite phase synthesized depends on each relaxor composition, namely on the different cations in the B^I site of the A(B^IB^{II})O₃ perovskite structure, such as Mg²⁺, Fe³⁺, Zn²⁺, Ni²⁺ and Co²⁺. The difference in the content of the perovskite phase for each relaxor could be attributed to the instability of the constituents in molten salts or their structural preference, i.e. strong covalency of ZnO in PZN [23]. Accordingly, PZN, PNN and PCN were not formed successfully by using the MSS. It is known that the three relaxors, PZN, PNN and PCN are difficult to form by a simple solid-state reaction.

The formation rate was also influenced by the type of salt as shown in Table II. In the case of PMN, the chloride flux was less effective than the sulphate flux in terms of perovskite phase formation. This is mainly due to the different melting points for each salt used. KCl, 0.5, NaCl–0.5 KCl and 0.635Li₂SO₄–0.365Na₂SO₄ have melting points of about 769, 650 and 594 °C, respectively. A high content (98%) of PMN phase was obtained at 750 °C in the case of the sulphate salts, which is below the melting point of PbO. It is plausible that the conventional problem of PbO evaporation can be reduced by using the MSS method. Although NaCl–LiCl salts have a low melting temperature of 600 °C, it is interesting to note that the perovskite phase was not formed. Several unknown phases were reported to be observed, possibly as a consequence of the reactions between the hygroscopic LiCl and the constituent oxides [24].

Another factor which can affect the reaction rate is the solubility of the oxides in the molten salt because the perovskite phase is believed to be formed on the surface of the slow-dissolving component by transporting the fast-dissolving component [1, 3, 9]. In the case of the lead-based relaxors, PbO is considered to be the fast-dissolving component [1, 3]. Therefore,

TABLE III Solubilities of PbO in various chloride and sulphate salts

Salts	Solubility (mol g ⁻¹ salt) for 2 h			
	750 °C	800 °C	850 °C	900 °C
KCl	1.1 × 10 ⁻⁵	–	1.9 × 10 ⁻⁵	–
KCl–NaCl	–	1.4 × 10 ⁻⁵	–	3.0 × 10 ⁻⁵
[3]				
Li ₂ SO ₄ ⁻	3.2 × 10 ⁻⁴	–	4.7 × 10 ⁻⁴	–
Na ₂ SO ₄				

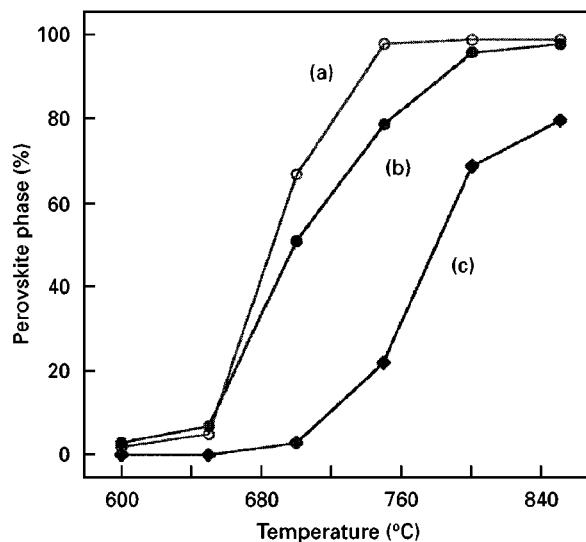


Figure 3 Variations in perovskite phase as a function of calcination temperature for powders prepared by MSS using (a) Li₂SO₄–Na₂SO₄, (b) KCl, and by (c) CMO.

the solubility of PbO in different salts can be used to explain the different contents observed in the perovskite phase. Table III shows the solubilities of PbO in different salts, indicating that the sulphates have higher solubilities of PbO under the same conditions than the chlorides. The higher solubility of PbO in the sulphates could be another reason for the higher content of PMN as shown in Table II.

Fig. 3 shows the variations in the perovskite PMN phase content with synthesis temperature according to the processing methods. When compared with the CMO method, the MSS utilizing sulphates or chloride was more effective in promoting the reaction of the PMN. Within a relatively narrow temperature range of 650–800 °C, the perovskite formation was complete in the case of the PMN–MSS due to the increased diffusivities of the constituents in the flux. It is noticeable that less than 80% perovskite phase was obtained even at a higher temperature of 850 °C in the CMO method. Above this temperature, the stoichiometry of PMN cannot be retained due to the evaporation of PbO.

Table IV shows the influence of other processing parameters on the formation of the perovskite phase in the case of the PMN using Li₂SO₄ and Na₂SO₄ salts. No considerable increase in the PMN content was observed beyond 5 min at 750 °C, indicating that the formation reaction in the MSS is very fast. The

TABLE IV Influence of processing parameters on the formation of perovskite PMN phases at 750 °C using $\text{Li}_2\text{SO}_4\text{-Na}_2\text{SO}_4$

Processing parameters	Conditions	Perovskite phase (%)
Heating time at 750 °C	5 min	97
	60 min	98
	120 min	98
	600 min	98
Molar ratio between Li_2SO_4 and Na_2SO_4	0.635–0.365	98
	0.27–0.71	91
	0.14–0.86	55
Weight ratio of salts to oxides, W	0.5	98
	1.0	98
	2.0	98
	3.0	97
Non-stoichiometric PMN	5 mol % excess MgO	100
	5 mol % excess PbO	99

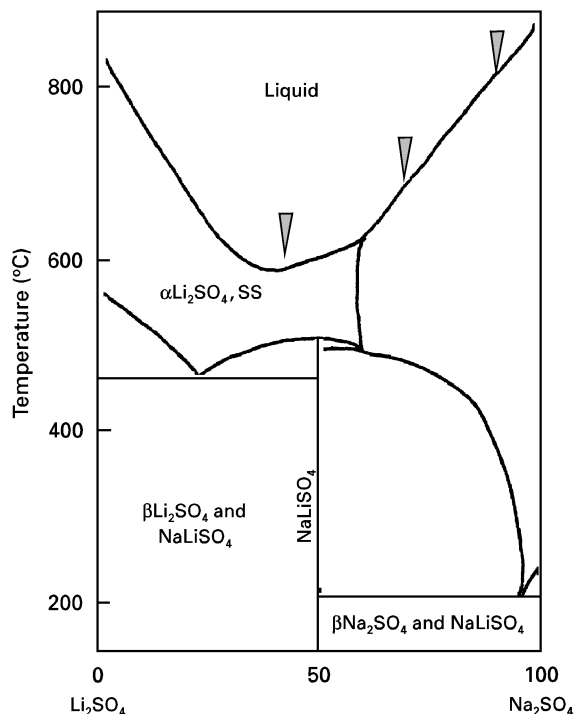


Figure 4 Phase diagram of the Li_2SO_4 and Na_2SO_4 system [25].

completion of the reaction in a very short time is due to the short diffusion distance and the high mobility of species in the liquid state. Arendt *et al.* [16], in an MSS study of PZT, reported that the mobilities in the liquid state can increase to 1×10^{-5} to $1 \times 10^{-8} \text{ cm}^2 \text{ s}^{-1}$; instead of $1 \times 10^{-18} \text{ cm}^2 \text{ s}^{-1}$ in the solid state. It should also be mentioned that the heating rate was not a significant factor in respect of the perovskite phase content.

The melting point of the salts can be varied by adjusting the different ratios of the two salts. For example, the melting point of the salts can be changed from 840 °C to 594 °C by increasing the molar ratio of $\text{Li}_2\text{SO}_4/\text{Na}_2\text{SO}_4$ from 0.14/0.86 to 0.635/0.365 as shown in the phase diagram of the Li_2SO_4 and Na_2SO_4 system (Fig. 4). The arrows in this figure indicate several salt compositions cited in this work. The different ratios influence the reaction rate of the perovskite phase significantly, as shown in

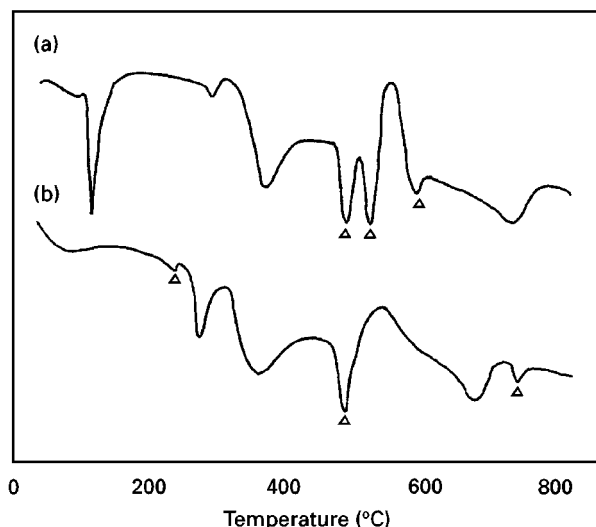


Figure 5 DTA curves of PMN prepared by MSS using (a) $0.635\text{Li}_2\text{SO}_4\text{-}0.365\text{Na}_2\text{SO}_4$ and (b) $0.29\text{Li}_2\text{SO}_4\text{-}0.71\text{Na}_2\text{SO}_4$.

Table IV. The eutectic composition of $0.635\text{Li}_2\text{SO}_4\text{-}0.365\text{Na}_2\text{SO}_4$ is found to be most effective in forming the PMN phase. The percentage of the perovskite phase was influenced very little by changing the relative amount of the salt to the oxides. Less salt is more advantageous experimentally because it is easier to separate the synthesized powders from the salt after cooling.

3. Phase stability in the molten salt

Phase stability is important in the MSS method because it affects the formation reaction and crystal structure [3, 18, 21, 26]. Thermal and chemical analyses, as well as phase identification, are the main tools used to investigate the stability of the perovskites in the molten salt.

Fig. 5 shows an example of the DTA curves of the PMN–MSS utilizing the two compositions of the sulphate salts. The arrows in this figure indicate the peaks corresponding to the phase transitions between the Li_2SO_4 and Na_2SO_4 salts. These peaks can be matched very well with the phase boundaries of each salt composition in the phase diagram of Fig. 4. This observation suggests that there is no side reaction between the salts and the constituent oxides, which can result in harmful second phases. Yoon *et al.* [18, 27] identified the phases present before washing, by X-ray diffraction (XRD) analysis. They concluded that there was no reaction product of the oxides and the salts in the case of PMN synthesis using sulphates or chlorides. In contrast, Chiu *et al.* [21] suggested that PFN synthesis using NaCl-KCl could be impeded by a reaction involving PbCl_2 as an intermediate phase, resulting in a potassium-substituted lead niobate compound. However, no experimental evidence was given.

Chemical analysis of the synthesized powder was performed using the atomic absorption (AA) and inductively coupled plasma (ICP) techniques to check the impurity levels originating from the salt used [1].

TABLE V Amounts (wt %) of impurities determined by AA and ICP analysis in the case of PMN using $\text{Li}_2\text{SO}_4\text{-Na}_2\text{SO}_4$ with variations in amount of salts

W^a	Li	Na	SO_4^{2-}
0.5	0.009	0.0290	0.038
3.0	0.011	0.0086	0.040

^a Weight ratio of salts to oxides.

Table V gives the chemical analysis results with variations in weight ratio, W , of the salts to the oxides in the case of PMN. Tiny amounts of the salt components are found to remain after the washing step. However, there was no tendency for the salt residues to increase with increasing relative amount of the salt to the oxides, W . The residues should be minimized through a careful washing treatment because these can degrade the dielectric properties and accelerate the aging rate if the impurities are substituted into the perovskite lattice in a considerable amount.

4. Morphological development and characteristics in the MSS

Typical micrographs of the PMN powder prepared by the sulphate MSS are shown in Fig. 6. An average particle size of around $0.5 \mu\text{m}$ with a relatively uniform size distribution can be obtained with a hold temperature of 750°C and time of 10 min by fast firing at a heating rate of $150^\circ\text{C min}^{-1}$ (Fig. 6a). There were no large agglomerates in this powder. When a normal heating rate of 5°C min^{-1} was used under the same conditions, the powder exhibited a larger average particle size, $\sim 1.5 \mu\text{m}$.

Isometric particles are found to exist in the sulphate MSS as shown in Fig. 6. With a prolonged synthesis time, faceting of the particles tended to occur in this case [1]. In the case of chlorides, the faceting was not found to be predominant even at a higher synthesis temperature [1, 28]. The deformation of the PMN crystallites was more extensive in the sulphate flux than in the chloride flux. It should also be noted that the particles obtained by the sulphate MSS were considerably larger than those obtained by the chloride MSS at the same amount of flux [1, 11]. The morphological difference can be explained by considering the crystallographic constraints given by the different sizes of the anions of the two salts [11]. Because Cl^{-1} and SO_4^{2-} ions move freely in the flux, each anion can influence the morphological development of the PMN particles. It is suggested that the growth of the PMN particles between the large sulphate ions progresses more rapidly than between the smaller chloride ions.

Generally, the particle of constituent oxides is developed in molten salts by two processes, the formation process and the particle growth process [1, 22]. As mentioned above, the formation process depends on the difference in dissolution rates between the reacting oxides in the molten salt. Because PbO is the fast-dissolving component in the lead-based niobates, the solubility of PbO in the sulphate and chloride flux

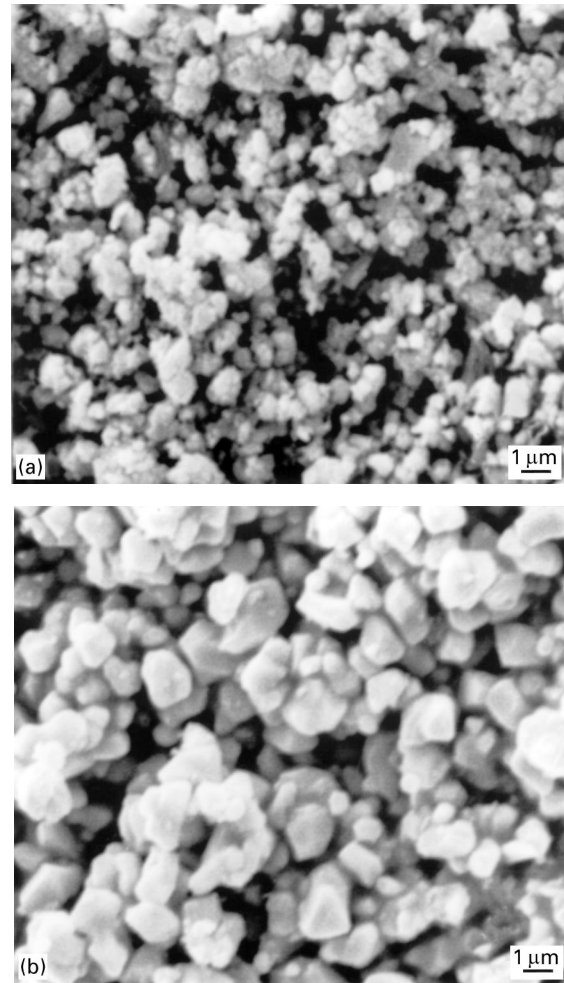


Figure 6 Scanning electron micrographs of PMN prepared at 750°C for 10 min by MSS using $0.635\text{Li}_2\text{SO}_4\text{-}0.365\text{Na}_2\text{SO}_4$, at a heating rate of (a) $150^\circ\text{C min}^{-1}$ and (b) 5°C min^{-1} .

should be considered in order to study the morphological difference of the PMN crystallites in both salts. With increasing temperature, the solubility of PbO increased more in the sulphate flux than in the chloride flux, as shown in Table III. The relatively large solubility of PbO in the sulphate flux increases the dissolution of PbO and then accelerates the formation reactions, resulting in changes in size and shape of the PMN particles [1]. Consequently, the PMN crystallites grown in the sulphate salts showed a larger particle size and somewhat faceted growth planes due to the larger solubility of PbO in the sulphate salts and the interaction between the cations of the oxides and the large sulphate anions.

The higher solubility in the case of the sulphates can also be responsible for the occurrence of extremely small particles attached to larger particles, which was found predominantly when a higher temperature or a larger amount of sulphate salts was applied [1, 19]. The particles were considered to be a perovskite phase [1]. The observed small particles suggest that there is another mechanism for perovskite formation in the MSS process; the dissolution-precipitation mechanism. The nuclei of the perovskite phase can be precipitated during cooling from the supersaturated constituents which were dissolved in the molten salt.

This phenomenon is believed to depend on the heating condition and the choice of salt.

There are many other factors which influence the morphological characteristics of the PMN phase as indicated in Table I. The particle size of the perovskite phase can be determined by changing the temperature, time and relative amount of salt. Interestingly, the PMN crystallite size was found to increase with increasing relative salt content, W [17]. These observations can be explained as being due to the increase in the solubility of PbO and in the space for particle growth, resulting from separating the reacting particles. The particle growth behaviour with temperature for the different amounts of salt can be represented by the following equation [29–32]

$$D^2 - D_0^2 = k(t - t_0) \exp(-E/RT) \quad (1)$$

where D is the average particle size at time t , D_0 is the initial particle size at initial time t_0 , k is the rate constant, E is the activation energy for particle growth, R is the gas constant, and T is the firing temperature. When the initial particle size, D_0 , is small compared with the average particle size, D , at the time t , the factor D_0^2 can be neglected relative to D^2 . From the plot of $\ln D^2$ versus $1/T$, the activation energy can be calculated. Fig. 7 shows the plots drawn for the PMN particles synthesized by changing the amount of the salts, $\text{Li}_2\text{SO}_4\text{--Na}_2\text{SO}_4$. The slopes of the straight lines indicate the activation energies for particle growth. There was no big difference in activation energy for two different amounts, $W = 0.5$ and 2.0 , of the sulphates. The activation energy values of $22\text{--}24 \text{ kcal mol}^{-1}$ were obtained for the MSS powders.

The effect of non-stoichiometry on the powder morphology was studied by adding excess PbO to PMN in the synthesis using the sulphate flux [1]. A small amount of excess PbO is needed to compensate for PbO loss during sintering. On increasing the amount of excess PbO from 1 mol % to 10 mol %, the particle size of PMN tended to decrease slightly. Rounded crystallites with no faceting were also observed with

the addition of excess PbO. This became more prominent as the amount of excess PbO increased, indicating that excess PbO tended to dissolve preferably the edges of the faceted PMN particles which were observed without excess PbO [1]. Therefore, it is believed that the edges of the PMN particle are more likely to form a smooth surface, resulting in a round particle.

5. Densification and dielectric properties of the MSS specimens

Densification behaviour has been studied for the lead-based niobates obtained by the MSS [19, 21, 33]. Shrinkage variations at an initial sintering temperature of 1000°C can be a good indication of the sinterability of the MSS powders, as shown in Fig. 8. It is noticeable that the line of the MSS powder, particularly in Fig. 8, is steeper than that of the CMO powder (Fig. 8a). From the different slopes of each line in this figure, it suggests that the sulphate MSS powders are more reactive than the CMO powders. The observed higher shrinkage values over the time range in the case of the CMO (Fig. 8a) can be attributed to the poor powder characteristics and the low purity of the perovskite phase [33]. Additionally, Fig. 8 shows the effect of the different particle sizes resulting from the two different amounts, $W = 0.5$ and 3.0 , of the sulphate salts. The average particle size was changed from $\sim 1.5 \mu\text{m}$ to $\sim 3.5 \mu\text{m}$ by increasing the salt amount from $W = 0.5$ to $W = 3.0$ at 750°C for 2 h. The case (Fig. 8b) of $W = 0.5$ is shown to be more effective in enhancing densification at the low temperature.

Several researchers have used the MSS method to improve the resultant microstructure and dielectric properties of lead-based relaxors [19, 33–38]. Generally, the dielectric properties of the relaxors depend on the microstructural characteristics such as grain size, grain-boundary character and pores. Therefore,

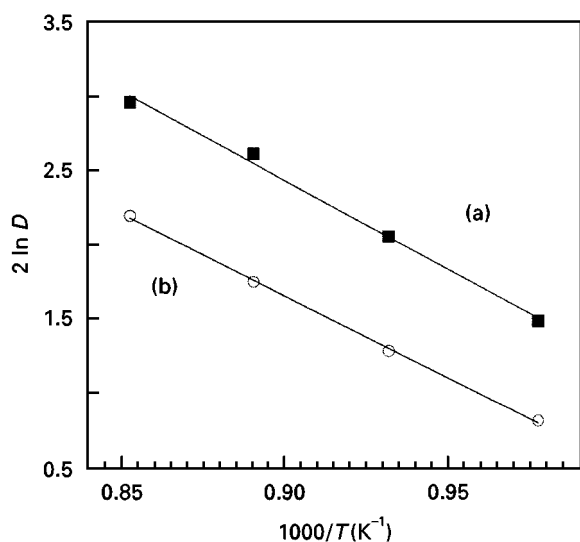


Figure 7 Plots of $2 \ln D$ (particle size) versus $1/T$ for (a) $W = 2.0$ and (b) $W = 0.5$ powders.

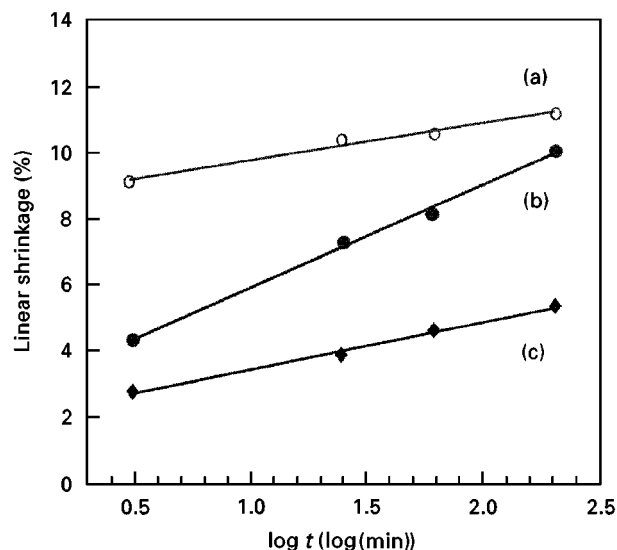


Figure 8 Shrinkage variations with time at a sintering temperature of 1000°C by (a) CMO, (b) $W = 0.5$ and (c) $W = 3.0$ by MSS, using $0.635\text{Li}_2\text{SO}_4\text{--}0.365\text{Na}_2\text{SO}_4$.

TABLE VI Compositions and dielectric constant of the lead-based relaxors prepared by the MSS method using chlorides or sulphates

Compositions	Synthesis conditions	Sintering conditions	Max. dielectric constant (1 kHz)	Reference
PMN	Li ₂ SO ₄ -Na ₂ SO ₄ W = 0.5, 750 °C/2 h	1200 °C/4 h	15 800	[34]
PMN	Li ₂ SO ₄ -Na ₂ SO ₄ W = 3.0, 750 °C/2 h	1200 °C/4 h	13 700	[34]
PMN with 3 mol % PbO	Li ₂ SO ₄ -Na ₂ SO ₄ W = 0.5, 750 °C/2 h	900 °C/4 h	15 000	[36]
0.9PMN-0.1PT ^a	KCl W = 0.7, 900 °C/1 h	1200 °C/3 h	25 000	[19]
0.9PMN-0.1PT with 2 mol % ZnO	NaCl-KCl W = 0.5, 750 °C/1 h	1100 °C/4 h	23 000	[37]
0.9PMN-0.1PT with 0.25 wt % V ₂ O ₅	NaCl-KCl W = 0.5, 750 °C/1 h	1100 °C/4 h	23 500	[38]
0.99PMN-0.01PMW ^b with 10 mol % MgO	NaCl-KCl W = 0.5, 700 °C/1 h	1150 °C/4 h	9 400	[39]

^a PbTiO₃.^b Pb(Mn_{2/3}W_{1/3})O₃.

microstructural control with an appropriate choice of additive can be critical in the applications. Better powder characteristics, such as a relatively uniform distribution of particle size and less particle agglomeration, obtained by using the MSS method, are believed to contribute to the resultant dielectric properties. Table VI summarizes the sintering conditions and dielectric constant values of various lead-based relaxors prepared with or without additives by the MSS method. Most of the results in Table VI demonstrate the good potential of the MSS method. Promising dielectric constant values were obtained at relatively low sintering temperatures in the MSS method. Homogeneous incorporation of the additives is expected in this method, as long as the additives are stable in the salts used, leading to the optimized performance of the additives even in relatively small amounts.

6. Conclusion

The MSS method utilizing a eutectic composition of 0.635Li₂SO₄-0.365Na₂SO₄ or 0.5NaCl-0.5KCl could be used successfully to prepare PMN and PFN without any detectable side products, as confirmed by thermal and phase analyses. The formation of a high-purity PMN phase occurred at a low temperature of 750 °C and was completed within a relatively narrow temperature range, leading to a small average particle size of ~0.5 μm with a controlled heating profile. Other processing parameters, such as the heating conditions, type and amount of salt, and non-stoichiometry, were responsible for differences in the content of the perovskite phase, the phase stability and the particle morphology characteristics. The observed different morphological characteristics according to different synthesis conditions can be explained possibly by the chemical and crystallographic constraints which were determined mainly by the molten salt environments, and the solubilities of the constituent oxides in the molten salts. Promising dielectric characteristics of the lead-based relaxors were believed to result from the better powder characteristics

induced by the MSS method. An understanding of the influences of the parameters is needed to control powder characteristics and to obtain a desirable result in the MSS of lead-based relaxors.

Acknowledgement

This work was supported by the Korea Science and Engineering Foundation through the CISEM at Yonsei University.

References

1. K. H. YOON, Y. S. CHO, D. H. LEE and D. H. KANG, *J. Am. Ceram. Soc.* **76** (1993) 1373.
2. T. KIMURA, M. H. HOLMES and R. E. NEWNHAM, *ibid.* **65** (1982) 223.
3. C. C. LI, C. C. CHIU and S. B. DESU, *ibid.* **74** (1991) 42.
4. K. NAGATA and K. OKAZAKI, *Jpn. J. Appl. Phys.* **24** (1985) 812.
5. K. H. YOON, K. Y. OH and S. O. YOON, *Mater. Res. Bull.* **21** (1986) 1429.
6. K. H. YOON and E. H. LEE, in "High Tech Ceramics", Materials Science Monographs 38B, edited by P. Vincenzini (Elsevier Scientific, Amsterdam, The Netherlands, 1987) p. 1873.
7. K. H. YOON, H. W. CHEONG, S. O. YOON and N. Y. LEE, *Mater. Res. Bull.* **23** (1988) 1527.
8. Y. ITO, S. SHIMADA and M. INAGAKI, *J. Am. Ceram. Soc.* **78** (1995) 2695.
9. Y. HAYASHI, T. KIMURA and T. YAMAGUCHI, *J. Mater. Sci.* **21** (1986) 757.
10. S. GOPALAKRISHNAN and W. A. SCHULZE, *Bull. Mater. Sci.* **14** (1991) 1157.
11. T. KIMURA and T. YAMAGUCHI, in "Ceramic Powders" (Elsevier Scientific, Amsterdam, The Netherlands, 1983) p. 555.
12. V. DANEK, L. SMUTNA and K. MATIASOVSKY, *Silikaty* **33** (1989) 97.
13. Y. HAYASHI, T. KIMURA and T. YAMAGUCHI, *J. Am. Ceram. Soc.* **69** (1986) 322.
14. S. OKAMOTO, Y. NARUMIYA and T. YAMAGUCHI, *Ceram. Int.* **12** (1986) 209.
15. K. H. YOON, D. H. LEE, H. J. JUNG and S. O. YOON, *J. Mater. Sci.* **27** (1992) 2941.
16. R. H. ARENDT, J. H. ROSOŁOWSKI and J. W. SZYMASZEK, *Mater. Res. Bull.* **14** (1979) 703.
17. K. H. YOON, Y. S. CHO, D. H. KANG, K. UCHINO and K. Y. OH, *Ferroelectrics* **160** (1994) 255.

18. K. H. YOON, Y. S. CHO and D. H. KANG, *J. Mater. Sci.* **30** (1995) 4244.
19. K. KATAYAMA, M. ABE and T. AKIBA, *J. Eur. Ceram. Soc.* **5** (1989) 183.
20. K. B. PARK and K. H. YOON, *Ferroelectrics* **132** (1992) 1.
21. C. C. CHIU, C. C. LI and S. B. DESU, *J. Am. Ceram. Soc.* **74** (1991) 38.
22. T. KIMURA and T. YAMAGUCHI, in "Advances in Ceramics", Vol. 21, Ceramic Powder Science, edited by G. L. Messing *et al.* (American Ceramic Society, Westerville, OH, 1987) p. 189.
23. T. R. GURURAJA, A. SAFARI and A. HALLIYAL, *Am. Ceram. Soc. Bull.* **65** (1986) 1601.
24. K. H. YOON, Y. S. CHO and D. H. KANG, unpublished work (1994).
25. A. NACKEN, *Neues Jahrb. Mineral. Ged. Beilage Bd.* **24A** (1910) 34.
26. S. GOPOLAKRISHNAN and W. A. SCHULZE, *Physica C* **229** (1994) 372.
27. K. H. YOON, C. K. KWAK and D. H. KANG, *Ferroelectrics* **87** (1988) 255.
28. K. KATAYAMA, M. ABE and T. AKIBA, *Ceram. Int.* **15** (1989) 289.
29. K. H. YOON, Y. S. CHO, Y. W. NAM and D. H. KANG, *J. Kor. Ceram. Soc.* **30** (1993) 543.
30. J. BURKE, *Trans. Am. Inst. Min. Metal. Eng.* **180** (1949) 73.
31. S. D. RAMAMURTHI, Z. XU and D. A. PAYNE, *J. Am. Ceram. Soc.* **73** (1990) 2760.
32. J. R. MACEWAN, *ibid.* **45** (1962) 37.
33. S. I. NUNES and R. C. BRADT, *ibid.* **78** (1995) 2469.
34. K. H. YOON, Y. S. CHO and D. H. KANG, *Ferroelectrics* **160** (1994) 89.
35. K. H. YOON, Y. S. CHO, D. H. LEE and D. H. KANG, in "Proceedings of the 9th Korea-Japan Seminar on New Ceramics", The Organizing Committee of The 9th Korea-Japan Seminar on New Ceramics (Seoul, Korea, 1993) p. 345.
36. *Idem*, *Ceram. Trans.* **41** (1994) 371.
37. K. H. YOON, Y. S. CHO and D. H. KANG, *Ferroelectrics* **146** (1993) 57.
38. *Idem*, *ibid.* **158** (1994) 417.
39. K. H. YOON, S. Y. KIM, Y. S. CHO and D. H. KANG, *J. Kor. Ceram. Soc.* **30** (1993) 629.

*Received 15 October 1997
and accepted 3 March 1998*